EFFECT OF IONIC LIQUIDS IN NANOPARTICLE SYNTHESIS: INTERACTION AND ORGANIZATION

Abstract

Ionic liquids (ILs) are becoming an innovatory synthesis medium for nanomaterials, permitting more efficient, safer, and environmentally friendly preparation of high-quality nanoparticles. Generally, stabilities of nanoparticles in ILs are emphasized as one of their outstanding advantages. ILs are employed as solvent for the of nanoparticles (NPs) as well as for surface functionalization. This chapter aims to cover in explaining the stabilities of NPs in imidazolium ILs using experimental as well as theoretical evidence. The synthesized NPs were characterized using SEM, HR-TEM, and UV-visible spectroscopic studies. A better understanding of interactions presents in imidazolium ILs explained using Density Functional Theory (DFT) and other theoretical calculations has been carried out. Interaction in various imidazolium ILs with nanoparticles has been deliberated using IR frequency calculation.

Keywords*: Ionic Liquids, Green reduction, Nanoparticle, DFT calculation.

Authors

Manju Kumari
Department of Chemistry
Maharaja college
Veer Kunwar Singh University
Ara, India
manjupandeya@gmail.com

Durga Gupta
Department of Chemistry
G.B. College Ramgarh Kaimur
Veer Kunwar Singh University
India

Madhulata Shukla
Department of Chemistry
G.B. College, Ramgarh, Kaimur
Veer Kunwar Singh University
India
madhu1.shukla@gmail.com

I. INTRODUCTION

Ionic liquids (ILs) are compounds mainly composed of organic cations and inorganic anions having melting points less than 100°C. In 1914, Ethyl ammonium nitrate was the first IL to be reported [1], who never realized that research on ILs will become such a broad field. Research on ionic liquids has been witnessing huge progress in the last 30 years. [2-13]. More than thousands of SCI papers are being published every year on ionic liquids. Room-temperature Ionic Liquids (RTILs) have reached extensive consideration as a solvent for synthesis as compared to hazardous and volatile organic solvents. Due to the non-volatile and non-flammable nature of RTILs, they are considered to be green solvents. [4-6] Also they can be recycled and reused again and again after the purification process. [10-11] ILs are considered new materials having very interesting properties. [12] ILs have also been termed designer solvents because of the flexibility of choosing different functional groups (shown in Figure 1) to synthesize many novel ILs for different purposes. From the last three decades, imidazolium ILs are the most studied and popular ILs. It is due to the fact that imidazolium ring attains the extra stability due to π- π interaction, their low viscosity, and also the process of synthesizing imimidazolium ILs are easy. [14-15] Several literatures are available to explain the application of imidazolium-based ILs as catalysts. [16-19]
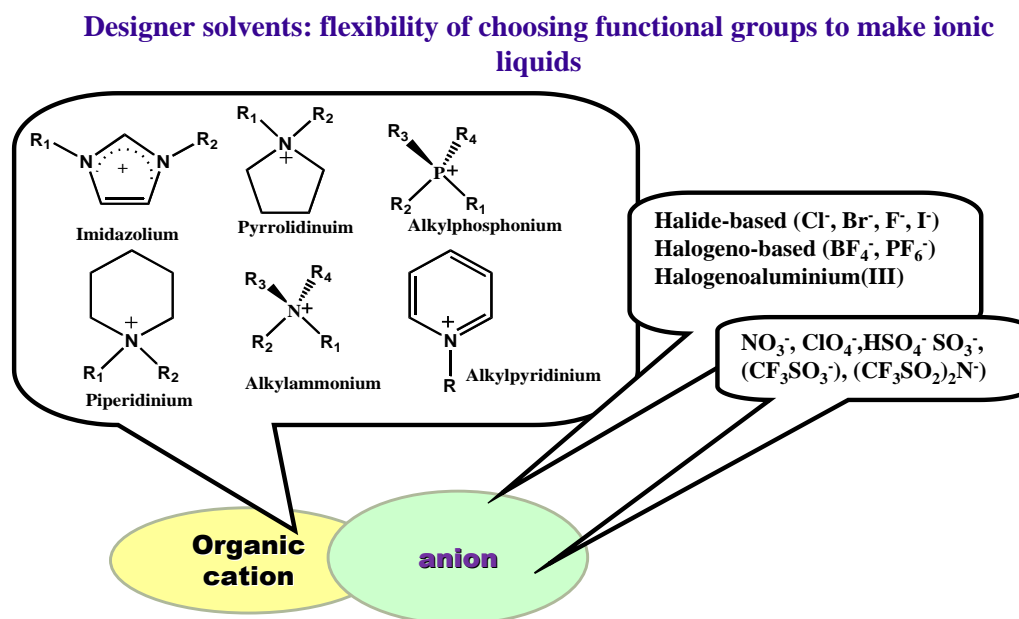
Designer solvents: flexibility of choosing functional groups to make ionic liquids

**Figure 1: Different combinations of ILs can be synthesized
By varying cat ions and anions.**

ILs are slightly exceptional to another organic solvents with respect to the formation of weak intermolecular weak hydrogen bonding along with ionic and covalent bond formation. [20-22] which are usually absent in other organic conventional solvents. The most challenging designs in ILs is the interionic interaction between the cations and anions through hydrogen bonding and also the position of anions which may be in plane or out of plane of the imidazole ring. [26-27] This discussion was fixed by recognizing the fact that imidazolium ring protons definitely perform as hydrogen bond donors, but only in the existence of adequately strong hydrogen bond acceptors [26-29] Most importantly, the above-

mentioned forces can control the physical properties of ILs, and consequently, ILs can be designed and prepared to obtain expected physical properties. [28-29] It is very essential to recognize the structural arrangement of ILs deeply, as physical and chemical properties are strongly dependent on the structure of the cationic and anionic arrangement. In this chapter, we can see that Imidazolium ILs had attracted ongoing interest, with most work focusing on structures, interactions present in them, and thermodynamic properties.

Nanoparticles (NPs) have a wide variety of potential applications as a result of their exceptional physical, chemical, optical, mechanical, and catalytic properties. Nanoparticles are ultrafine particles whose diameters are in the range of the nanometre scale. The properties of nanoparticles and their bulk are very much different from one another. Properties of NPs are characterized by their size, shape, structure, composition, crystallinity, etc. NPs can be synthesized via different modes such as chemical reduction, electroreduction, microwave, photochemical decomposition, etc. A huge amount of literature is available for Cu, Ag, and Au NPs, explaining the process of synthesis, its application, and its properties. [30-31] It is due to the fact that these elements exhibit well-localized surface plasmon resonance (LSPR) absorbance in the visible range. It also shows numerous catalytic applications in dark conditions as well as in the presence of light. Owing to the expensiveness of the gold and silver compounds, researchers are preferably using copper instead, for their research work.

Cu nanoparticles display greater electrical conductivity as well as catalytic action when compared with gold and silver. [32-33] CuNPs show LSPR absorbance in the visible range which is of low intensity. The main problem with CuNPs is that they are easily oxidized[34], still, copper oxide NPs have extensive use as catalysts in many of reactions. To enhance the photocatalytic properties of nanoparticles, bimetallic nanoparticles such as copper-silver nanoparticles or copper-gold NPs may be a technologically and economically useful decision. [35] A large surface-area-to-volume ratio leads to the unusual properties of nanoparticles.[36-38] Nanoparticles in ILs form crossbreed structures based on the different types of intermolecular as well as intramolecular structures formed across ILs and NPs. ILs acts as solvent medium in colloidal dispersals, [39] expediting the dispersal of metal nanoparticles [40], nanostructured inorganic particles [41], graphene [42], and carbon nanotubes [43-44]

Many of the nanoparticles can be suspended in ILs deprived of any additional stabilizers for example surfactants or polymers.[45] Electrostatic forces generated due to the cation-anion ion pair of ILs also impose on the NPs which act as stabilizers while synthesizing the nanoparticle in aqueous media. Considering IL as new material, several photocatalytic properties of numerous synthesized NPs are extensively being studied nowadays. Very few research papers are available explaining the stability of NP surface on its electronic properties of that kind of nanocomposites. Also, limited literature is available explaining the catalytic properties of these NPs. Recently published experimental and theoretical work explains that many macromolecules (except ILs) stabilizing nanoparticles also affect their electronic arrangements and their catalytic properties.[46] Tetrafluoroborate anion-based imidazolium- ILs i.e bmimBF4 are the mostly used ILs for the synthesis of NPs due to their stability and basic physical properties. [47] Theoretical calculations especially DFT calculation applied to recognize the mechanistic situations and to analyze the effect of ILs on the NPs. Limited reports are available explaining the synthesis and catalytic properties of Ag and Cu2O nanoparticles in 1-butyl-3-methyl imidazolium-based ILs. [48-50] This

chapter aims to summarize the Ag and Cu2O NPs synthesis in bmimBF4 IL using glucose as a reducing agent. Experimental as well as theoretical studies were carried out to investigate the interaction and orientation of cations and anions around the NPs. DFT calculations were executed to examine whether IL just acts as a stabilizer to prevent the aggregation of NPs clusters or also acts as an electron donor to activate the nanoclusters for further reaction. In our previously published research, we have discussed the better results obtained using B3LYP functional calculations which produce the stable cluster and also reproduce well with the experimental results obtained for IR and UV visible spectra. [51-52]

II. METHODOLOGY

AgNO₃ (Merck), Cu(NO3)₂.3H2O (Merck) bmimBF₄ (IoliTech), and glucose (Merck) chemicals were used for synthesizing silver and copper nanoparticles. All reagents were used as obtained without extra purification

Synthesis and characterization of Ag NP in bmimBF4 IL(Sample1)

A schematic diagram for the synthesis of silver NP in bmimBF4 IL is shown in **Scheme 1.1**. To synthesize Ag NP, 2 mL of 0.05 M AgNO₃ solution (in water) was taken in a round bottom flask and heated with constant stirring at 80°C. To this flask, 2 mL of 0.1 M, aqueous glucose solution was added dropwise. After 15 minutes of continuous stirring at 80°C, bmimBF4 IL (2 mL) was added dropwise to the above reaction mixture, and stirring continued for further 150 minutes at 105-110°C in an oil bath. After 3 hour of stirring, UV-visible spectrum was again recorded which indicate a peak shift from 430 nm (broad) to 423 nm which is found to be quite sharp peak, which suggests the formation of silver NP (AgNPs). AgNPs solution was light yellow in color in which silver nanoparticles of grey color are suspended in bmimBF4 IL. The resulting solution was kept under a vacuum to remove all the water molecules present in it. FTIR, NMR, and TEM used for further sample characterization.
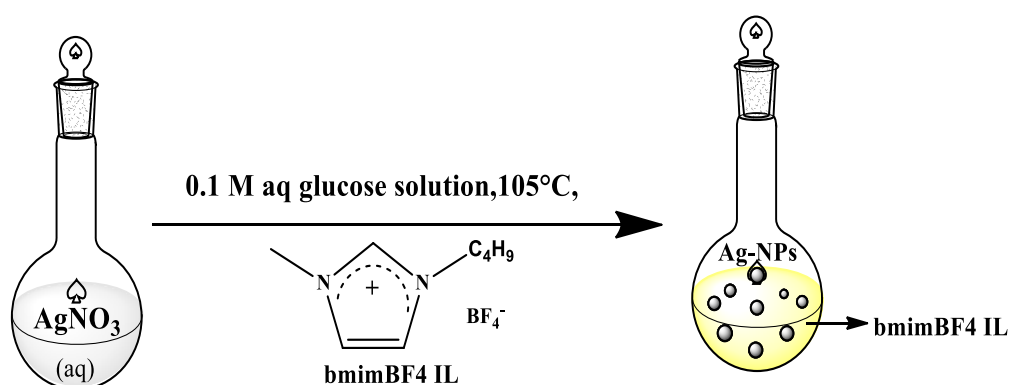

Scheme 1: Synthesis of Ag NP in 1-butyl-3-methylimidazolium tetrafluoroborate IL

Synthesis of cuprous oxide nanoparticles using bmimBF4 ionic liquid (Sample2)

Schematic diagram for the synthesis of Cu2O NP in bmimBF4 IL is shown in **Scheme 1.2**. 25mL of 0.1M Cu(NO3)₂.3H2O solution was placed in a RB flask. The reaction mixture was kept in a water bath whose temperature was maintained at 80°C. Dropwise 1mL (0.2 Mol/L) BMIMBF4 IL was added with continuous stirring. Stirring was continued for 20

minutes. 15mL of 0.5M Glucose was added with stirring at the same temperature. Stirring was done for 20 min at this temperature. The colour of the solution changes from blue to greenish-blue. After that 7mL 1M NaOH was added to gain the P^H approx. 11.5 stirring was done at the same constant temperature of 80°C for one and half hours. Colour of the solution changes to brown-yellow. The solution was centrifuged and the sample was washed well with ethanol. Dried in a acuum oven for 2 days. UV visible spectra were recorded and a sharp peak was observed at max 435nm and along with that, a broad spectrum was observed in the 494-541nm range wavelength. A sharp peak at 329nm corresponds to bmimBF4 IL.
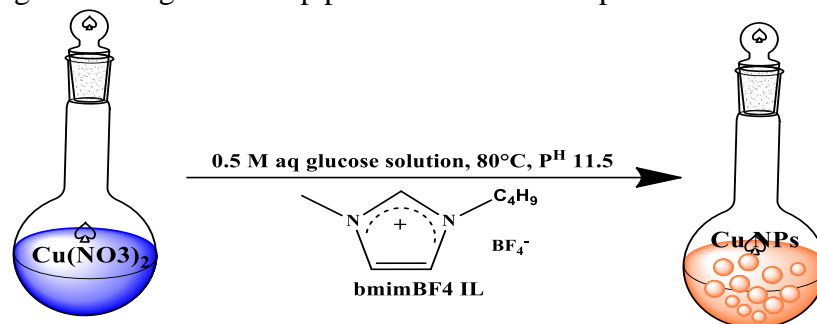
Scheme 1.2: Synthesis of cuprous oxide nanoparticle in bmimBF4

1. **Characterization:** Both the synthesized samples were characterized using X-ray diffraction technique, TEM, SEM and UV-visible spectroscopy.

2. **Computational Details:** MAPS software (Scienomics) was used to carve out the FCC Ag lattice and Cu_2O nanocluster. DFT calculations of clusters were carried out at B3LYP level [53-54] of calculation using Gaussian 16 program [55]. LANL2DZ basis set applied for Ag and Cu atoms [56] and 6-31G++(d,p) basis set used for C, N, H, O, F and B atoms. All the calculations were performed for ground state geometry optimization in the gaseous phase.

III. RESULTS AND DISCUSSION

1. **TEM measurements:** TEM image and electron diffraction pattern for AgNPs shows that particles with sizes ranging from 55 - 135 nm are formed. Due to the presence of Ag NPs in IL itself, all particles are associated with each other, as ILs are serving as associated medium between the NPs. Triangular, pentagonal, and hexagonal shaped nanoparticles are found to exist, as reported by us in our previous report. [45] Different shape and size of NPs are observed with the change of types of ILs as well as amount of ILs. Even small amount of impurity present in ILs changes the shape, size, and anisotropy of the NPs formed heavily. [57-58] TEM micrograph and electron diffraction pattern of synthesized Cu2O NPs shows particles with sizes varying from 11 - 15nm, reported by us in our earlier reports.[52]

2. **UV-visible and IR Spectroscopic studies:** UV-visible spectra of the Ag NPs in prepared in bmimBF4 shows a sharp absorbance peak at about 423 nm, as reported by us earlier. [45] This is a specific peak of the localized surface plasmon resonance (LSPR) absorption due to AgNPs. Cu_2O NPs prepared in bmimBF4 IL using protocol given in scheme 1.2 shows UV-visible spectrum with a sharp peak in the 300-350 nm region is due to

bmimBF4 IL and a broad peak in the 425-550nm range confirms Cu_2O NP synthesis. The same has been reported elsewhere [52]

The experimental IR spectrum of silver NPs in bmimBF4 IL has been compared with the IR spectra of pure bmimBF4 IL and found that the peak present at 850 cm^{-1} in pure IL redshifted to 833 cm^{-1} in the case of AgNPs associated with IL. Also, peaks at 1062 cm^{-1} in pure IL get red-shifted to 1028 cm^{-1} in Ag NP associated with bmimBF4 IL. The Ag-bmimBF4 product was more characterized using ^1H and ^{13}C NMR spectra and it has been found that there is no NMR peak shift observed when compared with NMR spectra of pure IL.[45] This clearly indicated that the Ag cluster is mostly surrounded by anions rather than cations. [59]

3. **Geometry Optimization:** Molecular geometry optimization of Ag13-2bmimBF4 and Cu2O-2bmimBF4 were carried out in the gas phase at the B3LYP level of calculation and using the Gaussian 16 program. Figures 6(a) and 6(b) represent the optimized geometry of Ag13-2bmimBF4 and Cu2O-2bmimBF4 respectively where different types of hydrogen bonding interactions are shown by the dotted line. Ag-Ag distance was found to be nearly between 2.80-3.0 The distance between Fluorine (BF4$^-$ anion of IL) and silver nanocluster is between 2.53-2.70 Å, which implies anions are much closer to nanocluster rather than cationic part. H----B-F hydrogen bonding distance found to be 2.28- 2.52 Å. BF4$^-$ anion interacts with different hydrogens of a methyl group, butyl group as well as hydrogens of imidazole ring, as reported by us in our previous research. [25] In the optimized structure of Cu2O-2bmimBF4, the distance between Fluorine (BF4$^-$ anion) and Cu_2O nanocluster is between 2.92-3.12Å. Cu-O distance found to be 1.84-1.86Å, H----B-F hydrogen bonding distance found to be 2.04- 2.62 Å. It is strongly supported from Figure 6 that more BF4 anions are localized around the Ag and Cu2O cluster instead of the imidazolium cation.
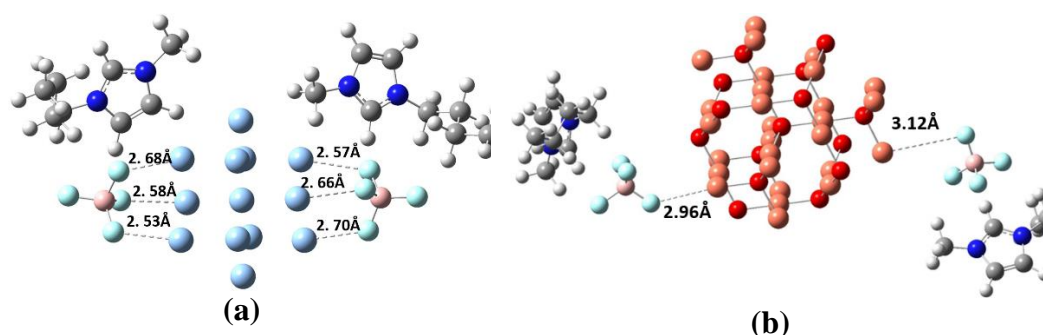
Figure 6: Optimized geometry of
(a) Ag13-2bmimBF4 and (b) Cu2O-2bmimBF4 moiety

4. **Mechanism for stabilizing metal NPs:** To stop the aggregation of synthesized NPs. stabilizing agents are added which generates a repulsive force that is necessary to provide stable metal NPs in the solution phase [60]. It states that stabilizing agents stabilize the metal NPs by passively synchronizing with them thus avoiding the agglomeration of NPs. Weak reducing agents play important role in controlling the shape and size of the NPs, whereas strong reducing agents didn't control the shape and size of synthesized NPs.[61] Several factors such as the use of type of metal salt precursors, reducing agents,

temperature, pH, etc. are responsible which controls the shape and size of the nanoparticles. Electrostatic, steric stabilization and a combination of both electrostatic and steric stabilization are three types of capping agents which affects the stabilization of metal NPs. [62]. Hydrogen bonding and van der Waals interactions play important role in determining the directionality of the interaction. [63] Several reviews provide a detailed use of imidazolium-based ILs (specifically) as stabilizing agents for metal NPs concerning their counteranions and exchange of their heteroatom.[64] ILs such as bmimPF6 and bmimBF4 are the most widely applied as a solvent for the synthesis of NPs and also used as stabilizing agents for the in situ synthesis of NPs [65].

It is expected from the previous research outcomes that the NPs were stabilized by the electrostatic interactions between the charged anionic and cationic moieties of ILs and metal atoms and also by the interaction between functionalized IL side chains (if present) and metal atoms. Therefore, the stabilization of metal NPs by ILs may not be only due to an electrostatic double-layer alone but may also be governed by weak attractive forces. [66] Just by a change in the counter anions only and cation remaining same or incorporation of different functional groups or substitutions at the cationic position of ILs when used as stabilizers results in varied applications of metal NPs. From the geometry optimization and Mulliken charge distribution (shown in Figure 7a and 7b for (a) Ag13-2bmimBF$_4$ and (b) Cu$_2$O-2bmimBF$_4$ respectively) calculation, it is very clear that anions are mainly localized around the nanoclusters and charges are present on the outermost surface of the nanoclusters, which is easily available for the catalytic activity.
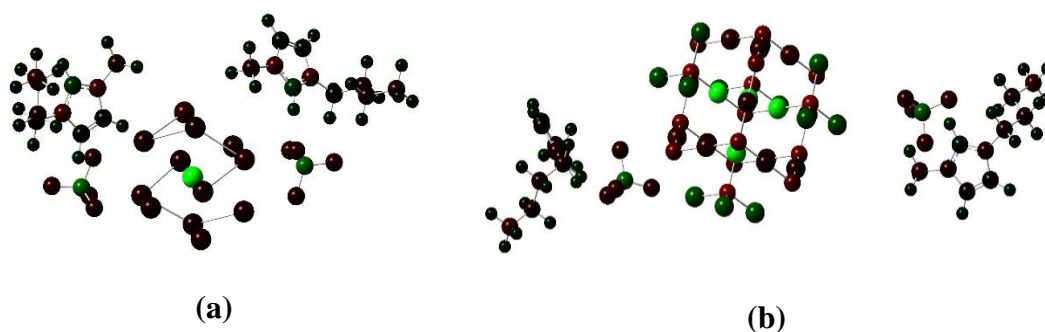

(a)   (b)

Figure 7: Mulliken charge distribution on
(a) Ag13-2bmimBF$_4$and (b) Cu$_2$O-2bmimBF$_4$ cluster showing the inner Ag and Cu atoms are extremely electropositive (light green coloured atoms)

Hence we can say that ILs not only effects the size and morphology of the NPs but it also activates the NPs by decreasing the band gap, as reported by us in our earlier research[45] Contour plot of HOMO and LUMO of Cu2O-2bmimBF4 nanocluster shown in Figure 8(a) and 8(b) respectively shows electron density is localized on Cu2O cluster. It is seen that it is localized on the Cu2O cluster only and not on the IL ion pairs. ILs just activate the Cu2O for further photocatalytic reactions. Also, ILs act as a stabilizer and solvent for the synthesis of nanoparticles. Many reports are available for the recyclability of the ILs and they can be reused for the other synthesis after further purification, as the catalyst could be easily separated from the reaction mixture without any significant loss in the catalytic activity.
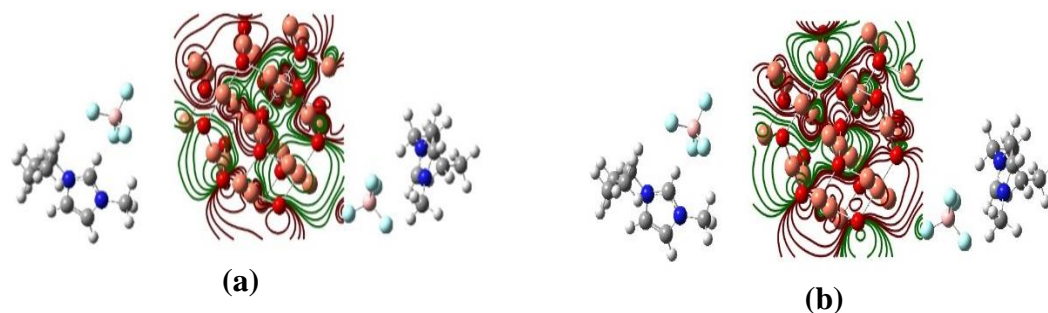
(a)　　　　　　　　　　　　　　　　(b)

Figure 8: HOMO - LUMO contour plot for Cu2O-2bmimBF4 IL nanocluster

Calculated IR spectra analysis: To better understand the ILs surroundings towards the silver nanoparticles and to analyse the strength of the bonding between the nanoclusters and the IL molecules, IR frequency calculations were carried out on the optimized geometry of bmimBF4 ion pair and Ag13-2bmimBF4 cluster using B3LYP level and same basis functions. The calculated frequency data for bmimBF4 ion pair and Ag13-2bmimBF4 cluster compared as follows. C2-H stretching occurring at 3273 cm^{-1} in bmimBF4 gets shifted to 3322 cm^{-1} in Ag13-2bmimBF4 cluster. 1075 cm^{-1} peak in bmimBF4 which is due to asymmetric B-F stretching coupled with C-N stretching gets shifted to 1060 cm^{-1} in Ag13-2bmimBF4. Scissoring of C-N-C in imidazole ring coupled with B-F asymmetric stretching occurs at 1016 which gets shifted to 1058 cm^{-1} in Ag13-2bmimBF4. Out of plane bending of C2-H in imidazole ring coupled with B-F asymmetric stretching found at 967 in bmimBF4 gets shifted to 1012 cm^{-1} in Ag13-2bmimBF4 cluster. Out of plane bending of C2-H in the imidazole ring of bmimBF4 occurs at 932, whereas it is found to exist at 953 cm^{-1} in Ag13-2bmimBF4 Also symmetric stretching of the B-F bond occurs at 842 cm^{-1} in bmimBF4, whereas it found to exist at 818 cm^{-1} in Ag13-2-bmimBF4.

842 and 1075 cm^{-1} peak shown in Figures 9(a) and 9(b) corresponds to symmetric and asymmetric B-F bond stretching respectively, which shows a red-shift of 24 and 15 cm^{-1} as shown in Figures 9(c) and 9(d) respectively. Experimentally, it was observed that two peaks present at 850 and 1062 cm^{-1} get in pure IL get red-shifted in AgNPs-IL. Hence one can conclude that the DFT calculated outcomes are proving the experimental observations to a large extent. C-H frequencies other than the C2-H frequency, do not have any significant variations. The calculated C2-H stretching frequency present at 3273 cm^{-1} in bmimBF4 (Figure **9(e)**) ion pair gets blue-shifted to 3322 cm^{-1} in Ag13-2bmimBF4 cluster (Figure **9(f)**). This specifies that the C2-H bond in IL is being affected by the silver cluster-IL interaction. Similarly, with Cu2O nanoclusters also, we can see from the optimized structure (Figure 6b) that Cu2O nanoclusters are surrounded mostly by BF4$^-$ anions rather than imidazolium cations. Strong interaction was found to exist between imidazolium cation and BF4 anion ion pair when in isolated form, but the strength of interaction between cation and anion decreases when anion interacts with silver NPs. It was observed from the calculated frequency that other than C2-H stretching frequency, others remain unaffected. Hence it clearly indicates that the anionic part is interacting with the silver clusters.
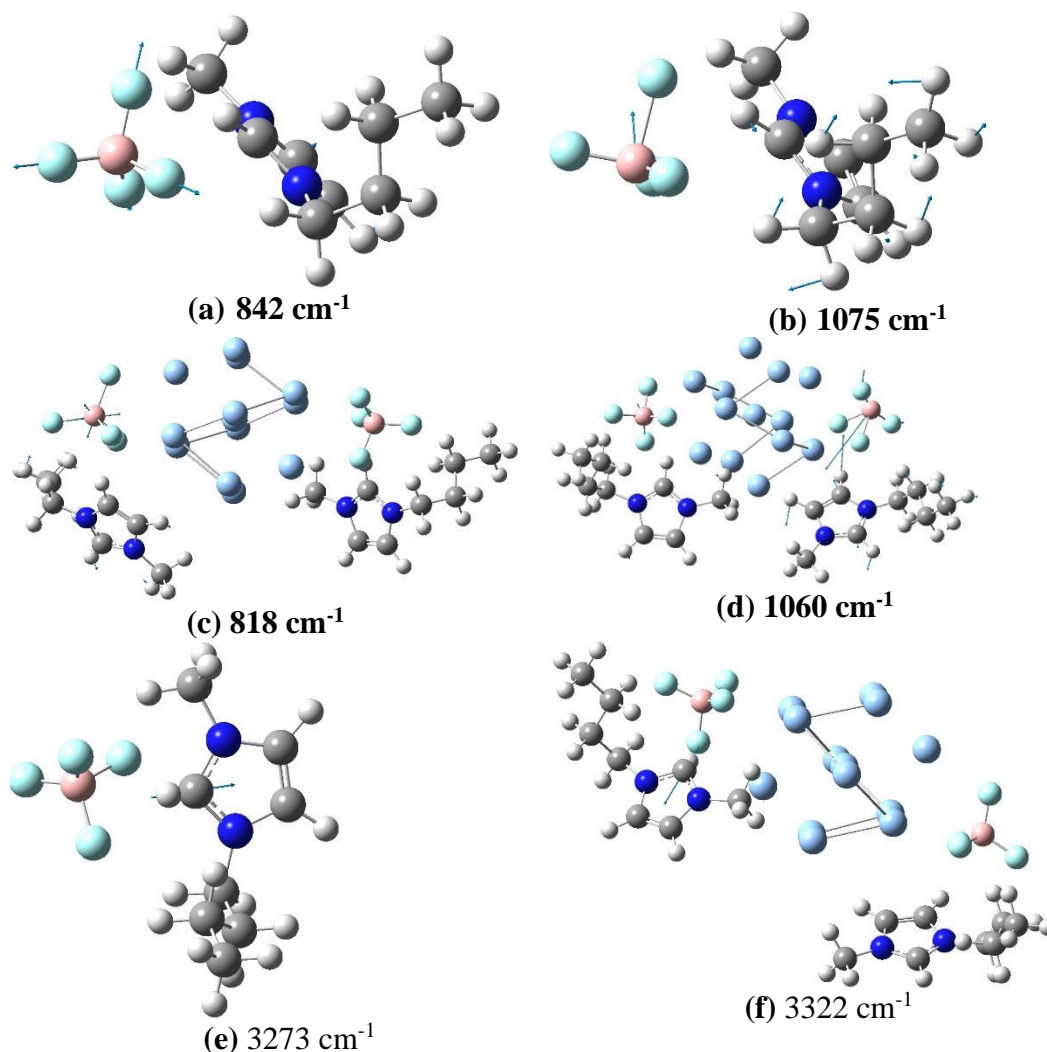
(a) 842 cm^{-1}

(b) 1075 cm^{-1}

(c) 818 cm^{-1}

(d) 1060 cm^{-1}

(e) 3273 cm^{-1}

(f) 3322 cm^{-1}

Figure 9: Different stretching frequencies of bmimBF4 ion pair and Ag13-2bmimBF4 cluster. Displacement is shown by calculated eigenvectors (the blue arrow represents the direction of atomic displacement).

IV. CONCLUSIONS

Green synthesis of silver and copper (I) oxide nanoparticles in bmimBF4 IL has been accomplished using glucose as the reducing agent. The reaction was found to be completed in very less time (3 hours) violating all the ideas of green synthesis procedures for which a long duration is required for synthesis. Anisotropic AgNPs with varying shapes such as triangular, pentagonal, and hexagonal have been reported. Cu2O NPs are in the 11 - 15nm range with hollow spherical shapes. The insignificant shift in ^{1}H NMR for Ag NPs specifies that the IL molecules associated with the nanoclusters through their anionic part and hence stabilizing the nanoparticle. Stretching frequencies associated with the anion of the pure IL show red-shift when bmimBF4 IL is associated with silver nanocluster. The effect of IL on Ag and Cu$_2$O nanoparticles has been better explained using DFT calculations. Molecular geometry optimization results observed from DFT calculations help in understanding the stabilization mechanism better. The optimized geometry of both the nanoclusters attained using DFT calculation demonstrates that nanoclusters interact with IL through their anionic site. The

theoretically observed IR data strongly proves this conclusion. Mulliken charge distribution calculation shows that anions are mainly localized around the nanoclusters and charges are present on the outermost surface of the nanoclusters, which is easily available for catalytic activity. Research outcomes show electrostatic interactions between the charged anionic and cationic moieties of ILs and metal cluster stabilizes the NPs.

Declaration of conflict of interests
The authors declare no conflict of interest.

REFERENCES

[1] P. Walden, *Bull. Acad. Imp. Sci. St. Petersburg*, Ser. **8** (1914) 405.
[2] K. R. Seddon, *Nature Mater.* **2** (2003) 363.
[3] P. Wasserscheid and W.Keim, *Angew. Chem. Int. Ed.* **39** (2000) 3772.
[4] R. D. Rogers and K. R. Seddon, *Science* **302** (2003) 792.
[5] H. Ohno, *in* "Ionic liquids: The Front and Future of Material Developments", CMC press, Tokyo, 2003.
[6] M. Shukla, S. Saha, *Comput. Theor. Chem.* **1015** (2013) 27.
[7] A. Paul and A. Samanta, *J. Phys. Chem. B* **111** (2007) 4724.
[8] H. C. Chang, J. C. Jiang, C. Y. Chang, J. C. Su, C. H. Hung, Y. C. Liou, and S. H. Lin, *J. Phys. Chem. B* **112** (2008) 4351.
[9] S. Patra and A. Samanta, *J. Phys. Chem. B* **116** (2012) 12275.
[10] K. Santhosh, and A. Samanta, *J. Phys. Chem. C* **116** (2012) 20643.
[11] K. Iwata, H. Okajima, S. Saha and H. Hamaguchi, *Acc. Chem. Res.* **40** (2007) 1174.
[12] J. N. A. C. Lopes and A. A. H. Pádua, *J. Phys. Chem. B.* **110** (2006) 3330.
[13] M. Shukla, S. Saha, in *Ionic Liquids - New Aspects for the Future*" InTech Publication (2013**)** *pp* 61-84
[14] *D. Weingarth, I. Czekaj, Z. Fei, A. Foelske-Schmitz, P. J. Dyson, A. Wokaun and R. Kötz, J. Electrochem. Soc*., **159** (2012) 611-615.
[15] C. Wang, H. Luo, X. Luo, H. Li and S. Dai*, Green Chem., 12 (2010) 2019.*
[16] J. S. Ghomi, A. R. Hajpour, M. Emaeili, *Digest J. Nanomaterials and Biostruct.* **5** (2010) 865.
[17] J. I. Yu, H. Y. Ju, K. H. Kim and D. W. Park, *Korean J. Chem. Engineer.*, **27** (2010) 446.
[18] A. Sarkar, S. R. Roy, N. Parikh and A. K. Chakraborti, *J. Org. Chem.*, **76** (2011) 7132.
[19] D. Sarkar, R. Bhattarai, D. A. Headley and B. Ni, *Synthesis*, **12** (2011) 1993.
[20] J. Dupont, *J. Braz. Chem. Soc.* **15** (2004) 341.
[21] S. Saha and H. Hamaguchi, *J. Phys. Chem. B.* **110** (2006) 2777.
[22] S. Saha, S. Hayashi, A. Kobayashi, and H. Hamaguchi, *Chem. Lett.* **32** (2003) 740
[23] M. Shukla *J. Mol. Struc.* **1131** (2017) 275.
[24] M. Shukla, N. Srivastava and S. Saha *J. Mol. Struc.* **975** (2010) 349.
[25] M. Shukla, N. Srivastava, S. Saha, *in Ionic Liquids-Classes and Properties* InTech Publication, (2011**)** *pp* 153.
[26] R, Lungwitz, S. Spange *Chem. Phys. Chem.* **13** (2012)1910.
[27] P. A. Hunt *Top Curr. Chem.* **375** (2017) 59.
[28] A. Elaiwi, P. B. Hitchcock, K.R Seddon, N. Srinivasan, Y. M. Tan, T. Welton, J. A. Zora *J Chem Soc Dalton Trans* (1995) 3467.
[29] M. Shukla, H. Noothalpati, S. Shigeto, S. Saha, *Vib. Spect.***75** (2014) 107.
[30] K.G. Stamplecoskie, J. Scaiano, *J. Phys. Chem. C* **115** (2011) 1403.

[31] X. C. Duan, J. M. Ma, J. B. Lian, W. J. Zheng, *Cryst Eng. Comm* **16**, (2014) 2550.

[32] C. S. Choi, Y. H. Jo, M. G. Kim, H. M. Lee, *Nanotechnology* **23** (2012) 065601.

[33] T. Wu, Q. Huang, W. Li, G. Chen, X. Ma, G. Zeng, *Journal of Nanomaterials* 2014, Article ID 751424, 6 pages.

[34] A. Muzikansky, P. Nanikashvili, J. Grinblat, D. Zitoun, *J. Phys. Chem. C* **117** (2013) 3093.

[35] K. Shin, D. H. Kim, S. C. Yeo, H. M. Lee, *Catal. Today* **185** (2012) 94.

[36] A. N. Shipway, E. Katz, I. Willner, *Chem. Phys. Chem.* 1 (2000) 18.

[37] P. K. Jain, X. H. Huang, I. H. El-Sayed, M. A. El-Sayed, *Acc. Chem. Res.* **41** (2008) 1578.

[38] H. Wender, P. Migowski, A. F. Feil, S. R. Teixeira, J. Dupont, *Coord. Chem. Rev.* **257**, (2013) 2468-2483.

[39] K. Ueno, M. Watanabe Langmuir 27 (2011), 9105.

[40] G. S. Fonseca, G. Machado, S. R. Teixeira, G. H. Fecher, J.Morais, M. C. M. Alves, J. Dupont, *J. Colloid Interface Sci.* **301** (2006), 193.

[41] Y. Zhou, M. Antonietti, *J. Am. Chem. Soc.* **125** (2003) 14960.

[42] S. Ravula, S. N. Baker, G. Kamath, G. A. Baker, Nanoscale **7** (2015) 4338.

[43] Y. Shim, H. J. Kim, *ACS Nano* **3** (2009) 1693.

[44] T. Fukushima, A. Kosaka, Y. Ishimura, T. Yamamoto, T. Takigawa, N. Ishii, T. Aida, *Science* **300** (2003) 2072.

[45] M. Shukla, A. Verma, S. Kumar, S. Pal, I. Sinha Heliyon 7, **2021**, e6065.

[46] M. Shukla, I. Sinha *Int. J. Quantum Chem.* **2018**; e25490 doi.org/10.1002/qua.25490.

[47] T. A. Kareem, A. A. Kaliani, *Arabian j. Chem.* **12** (2019) 2810.

[48] W. Wang, X. Peng, H. Xiong, W. Wen, T. Bao, X. Zhang and S. Wang *New J. Chem.*, 2017, 41, 3766.

[49] K. W. Araneda, C. Valdebenito, M. B. Camarada, G. Abarca, D. C. Arriagada *J. of Mol. Liquids* **310** (2020) 113089.

[50] C. M. Correa. M. A. Bizeto, F. F. Camilo *J Nanopart Res* **18** (2016) 132.

[51] A. Verma, R. K. Gupta, M. Shukla, M. Malviya, I. Sinha *J. Nanosci. Nanotechnol.* **20** (2020).

[52] M. Shukla, S. Pal, I. Sinha *J. Mol. Struct. 2022* doi.org/10.1016/j.molstruc.2022.132961**.**

[53] C. Lee, W. Yang, R. G. Parr *Phys. Rev. B***,** *37* (1988) 785.

[54] A. D. Becke *J. Chem. Phys.* **98** (1993) 5648.

[55] M. J. Frisch, G. W. Trucks, H. B. Schlegel, G. E. Scuseria, M. A. Robb, J. R. Cheeseman, G. Scalmani, V. Barone, G. A. Petersson, H. Nakatsuji, X. Li, M. Caricato, A. V. Marenich, J. Bloino, B. G. Janesko, R. Gomperts, B. Mennucci, H. P. Hratchian, J. V. Ortiz, A. F. Izmaylov, J. L. Sonnenberg, D. Williams-Young, F. Ding, F. Lipparini, F. Egidi, J. Goings, B. Peng, A. Petrone, T. Henderson, D. Ranasinghe, V. G. Zakrzewski, J. Gao, N. Rega, G. Zheng, W. Liang, M. Hada, M. Ehara, K. Toyota, R. Fukuda, J. Hasegawa, M. Ishida, T. Nakajima, Y. Honda, O. Kitao, H. Nakai, T. Vreven, K. Throssell, J. A. Montgomery, Jr., J. E. Peralta, F. Ogliaro, M. J. Bearpark, J. J. Heyd, E. N. Brothers, K. N. Kudin, V. N. Staroverov, T. A. Keith, R. Kobayashi, J. Normand, K. Raghavachari, A. P. Rendell, J. C. Burant, S. S. Iyengar, J. Tomasi, M. Cossi, J. M. Millam, M. Klene, C. Adamo, R. Cammi, J. W. Ochterski, R. L. Martin, K. Morokuma, O. Farkas, J. B. Foresman, and D. J. Fox, Gaussian, Inc., Wallingford CT, 2016.

[56] P. J. Hay, W. R. Wadt *J. Chem. Phys.* **82** (1985) 270.

[57] F. Samari, S. Dorostkar *J. Iran Chem Soc.***13** (2016) 689.

[58] J. B. Chang, C. H. Liu, J. Liu, Y.Y. Zhou, X. Gao, S. Dong W. *Nano. Micro Lett.* **7 (2015)** 307.

[59] C. Janiak *Review Ionic Liquids for the Synthesis and Stabilization of Metal Nanoparticles Z. Naturforsch.* **68b** (2013) 1059.

[60] D Astruc Nanoparticles and catalysis. *Wiley Online Library, Weinheim* (2008).

[61] Y Qin, X Ji, J Jing, H Liu, H Wu, W Yang *Colloids Surf A* **372** (2010) 172.

[62] D P Stankus, S E Lohse, J E Hutchison, J A Nason *Environ Sci Technol* **45** (2010) 3238.

[63] M Antonietti, D Kuang, B Smarsly, Zhou *Angew Chem Int Ed* **43** (2004) 4988.

[64] K. Manojkumar, A. Sivaramakrishna, K. Vijayakrishna *J Nanopart Res***18** (2016) 103.

[65] B Mohan, H Woo, Jang S, Lee S, Park S, Park KH *Solid State Sci* **22** (2013)16.

[66] H   Zhang,   H   Cui   *Langmuir*   **25**   (2009)   2604.